Simulation of Electric Field and Potential Distributions on Silicone Rubber Polymer Insulators under Contamination Conditions Using Finite Element Method

BOONRUANG MARUNGSRI and WINAI ONCHANTUEK
Alternative and Sustainable Energy Research Unit, Power and Control Research Group
School of Electrical Engineering, Institute of Engineering, Suranaree University of Technology
Muang District, Nakhon Ratchasima, 30000, THAILAND
Email: bmshvee@sut.ac.th , kimhunwu_ee10@hotmail.com

Abstract: - This paper presents the simulation results of electric field and potential distributions along surface of silicone rubber polymer insulators under clean and contamination conditions. In former experimental research, silicone rubber polymer insulators having near the same leakage distance are subjected to 15 kV during 50 test cycles of artificial salt fog ageing test. After 50 test cycles, alternate sheds silicone rubber polymer insulator showed better contamination performance than straight sheds silicone rubber polymer insulator. Severe surface ageing was observed on the straight sheds insulator. The objective of this work is to elucidate that electric field distribution along straight sheds insulator higher than alternate shed insulator in salt fog ageing test. Finite element method (FEM) is adopted for this work. The simulation results confirmed the experimental data, as well.

Key-Words: - Electric field distribution, potential distribution, silicone rubber polymer insulator, straight sheds, alternate shed, clean condition, contamination condition, finite element method

1 Introduction

Polymer insulators, which are being used increasingly for outdoor applications, have better characteristics than porcelain and glass types: they have better contamination performance due to their surface hydrophobicity, lighter, possess higher impact strength, and so on. However, since polymer insulators are made of organic materials, deterioration through ageing is unavoidable. Hence, ageing deterioration is a primary concern in the performance of polymer insulators. Artificial salt fog ageing tests have been most widely conducted on simple plates, rods, and small actual insulators for evaluating the anti-tracking and/or anti-erosion performance of housing materials for polymer insulators [1–8].

Structure of a polymer insulator is shown in Fig. 1. The basic design of a polymer insulator is as follows; A fibre reinforced plastic (FRP) core, attached with two metal fittings, is used as the load bearing structure. The presence of dirt and moisture in combination with electrical stress results in the occurrence of local discharges causing the material deterioration such as tracking and erosion. In order to protect the FRP core from various environmental stresses, such as ultraviolet, acid, ozone etc. and to provide a leakage distance within a limited insulator length necessary under contaminated and wet conditions, weather sheds are installed outside the FRP core. Silicone rubber is mainly used for polymer insulators or composite insulators as housing material.[9]

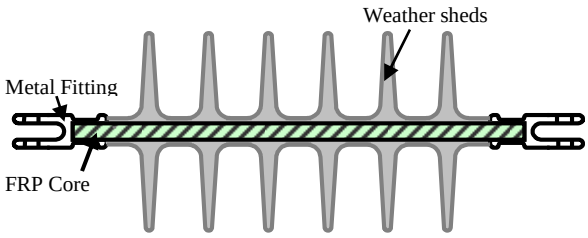

Fig. 1 Structure of a Polymer Insulator

In previous work, salt fog ageing test have been conducted on specimens having different configurations [10]. Although tested specimens having the same leakage distance and made of the same material, obviously degree of surface ageing on tested specimens was obtained. Fully results and discussions are found in [10]. However, briefly results are illustrated in Section 2.

2 Problem Formulation

Two insulator-type specimens, having straight and alternate sheds, were prepared as shown in Fig. 2. All the specimens were made of high-temperature vulcanized silicone rubber (HTV SiR) with alumina trihydrate (ATH: $Al_2O_3 \cdot 3H_2O$) filler contents of 50 parts per 100 by weight (pph). The insulator-type specimens were prepared by molding HTV SiR onto the FRP rods. Molding lines or parting lines were found on these insulator-type specimens. Two pieces of each specimen type were used in this investigation. All specimen surfaces were cleaned by ethyl alcohol 24 hours before starting the test.

All specimens were hung vertically in a plastic chamber as shown in Fig. 3 and were tested together under the test conditions shown in Table 1. The cyclic salt fog ageing test was conducted by injecting salt fog into the chamber for 8 hours and stopping it for 16 hours every day under AC 15kV. The salt fog, with a salinity of 800 μS/cm and an injection rate of 0.5 l/hr/m^3, was generated using an ultrasonic humidifier and was injected from the top of the test chamber as shown in Fig. 3. Leakage currents were continuously measured on individual specimens.

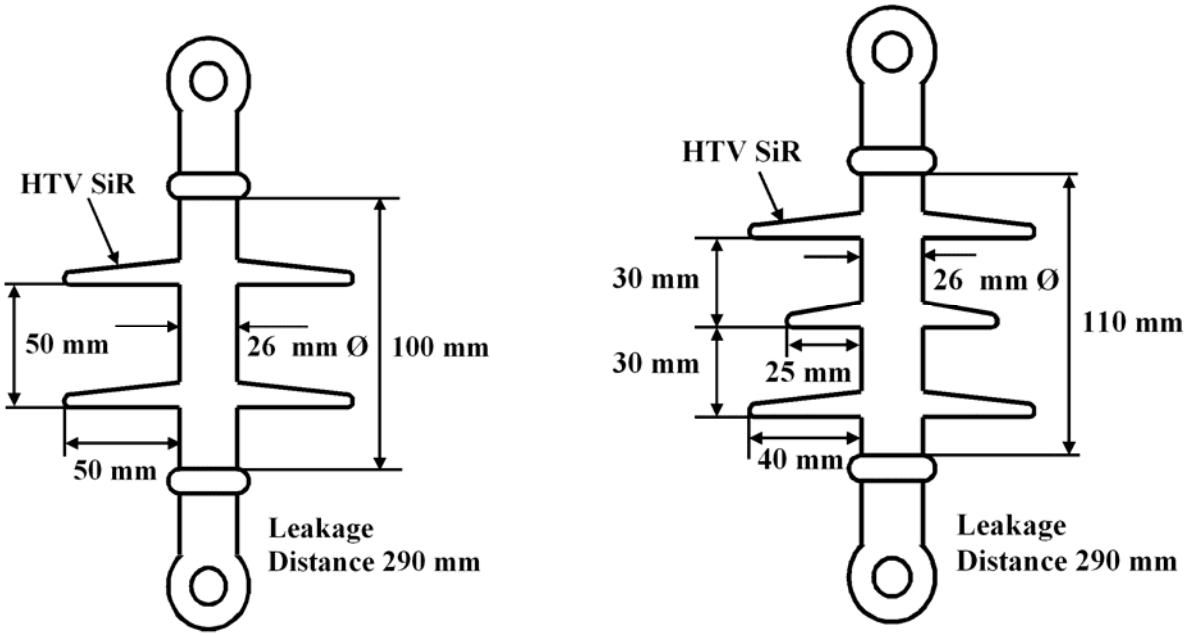

(a) Straight Shed (b) Alternate Shed

Fig.2 Test Specimens

Table 1 Test Conditions

Test Chamber		1590 mm×1560 mm ×1330H mm, (2m3)
Test Voltage		AC 15 kV, Continuously Applied
Voltage Stress		60 V/mm for rod type, 51.3 V/mm for insulator types
Salt Fog	Generation	Ultrasonic Humidifier (Model WM – B NB 1000)
	Injection Rate	0.5 l / hr / m3
	Conductivity	800 μS / cm
Test Sequence in 1 Cycle (24 hours)		Salt fog injected for 8 hours and stopped for 16 hours

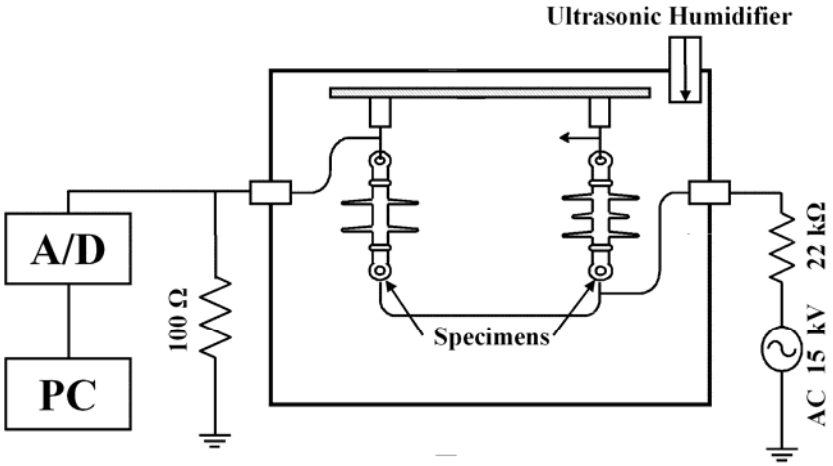

Fig. 3 Test Arrangement.

During 50 test cycle of salt fog ageing test, stronger surface discharges were observed on the specimen having straight sheds comparing with the specimen having alternate sheds although all specimens having the same leakage distance and made of the same materials. The observation result is illustrated in Fig. 4. After 50 test cycles, severe surface ageing was observed on the trunk between sheds of specimens having straight shed comparing with the specimen having alternate sheds, as shown in Fig. 5. Considering the results, the assumption is electric filed distribution along the specimen having straight shed higher than the specimen having alternated sheds.

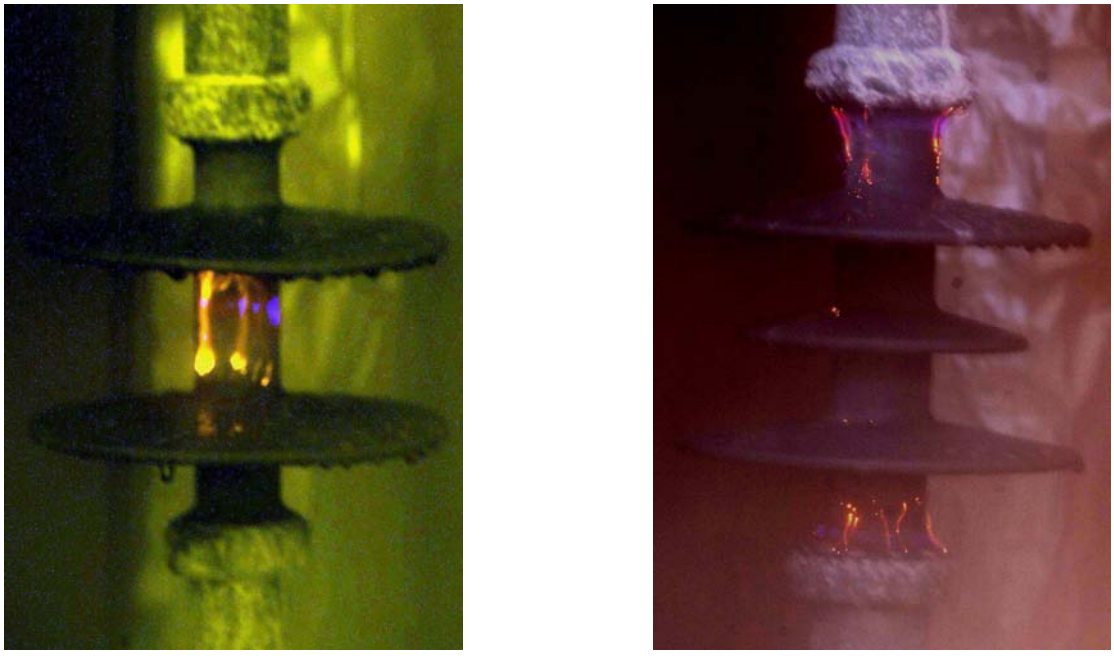

(a) Straight Shed (b) Alternate Shed

Fig. 4 Discharge on Specimen Surface during 50 Test Cycles.

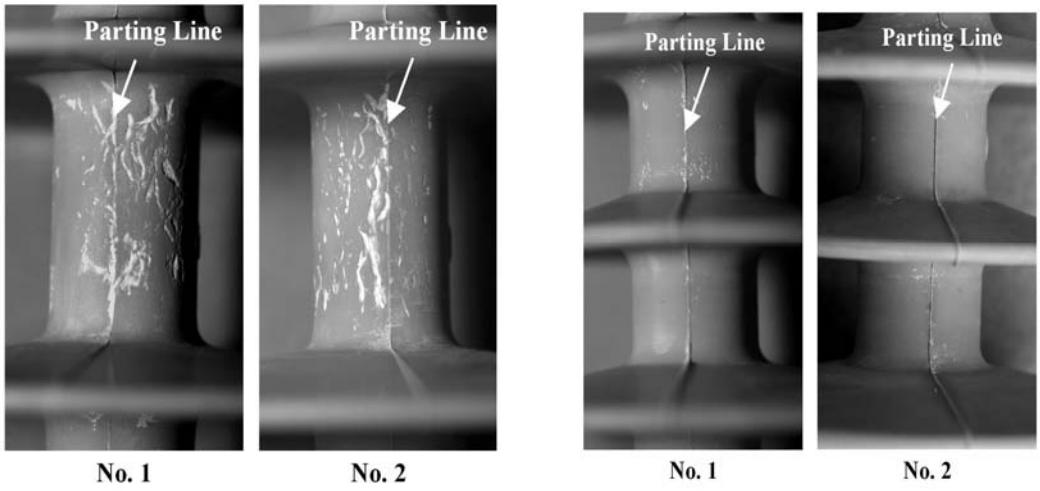

(a) Straight Shed (b) Alternate Shed

Fig. 5 Ageing of Specimen Surface after 50 Test Cycles

3 Problem Solution

3.1 Equations for Electric Field and Potential Distributions Calculation

Simply way for electric field distribution calculation is calculate electric potential distribution. Then, electric field distribution is calculated by minus gradient of electric potential distribution. Due to electrostatic field distribution, electric field distribution can be written as follows [11]:

$$E = -\nabla V \tag{1}$$

From Maxwell's equation

$$\nabla E = \frac{\rho}{\varepsilon} \tag{2}$$

where ρ is resistivity Ω/m,

ε is dielectric constant of dielectric material ($\varepsilon = \varepsilon_0 \varepsilon_r$)

ε_0 is air or space dielectric constant (8.854×10^{-12} F/m)

ε_r is relative dielectric constant of dielectric material

Place equation (1) in equation (2) obtained Poisson's equation.

$$\nabla \varepsilon \nabla V = -\rho \tag{3}$$

Without space charge ($\rho = 0$), Poisson's equation becomes Laplace's equation.

$$\nabla \varepsilon \nabla V = 0 \tag{4}$$

3.2 Equations for FEM Analysis of the Electric Field Distribution

The finite element method is one of the numerical analysis methods based on the variation approach and has been widely used in engineering problems, i.e. electric and magnetic field analyses, mechanical and thermal analyses, since the late 1970s [12–15]. Supposing that the domain under consideration does not contain any space and surface charges, the two-dimensional functional $F(u)$ in the Cartesian system of coordinates can be written as follows[16]:

$$F(u) = \frac{1}{2}\int_D \left[\varepsilon_x \left(\frac{du}{dx}\right)^2 + \varepsilon_y \left(\frac{du}{dy}\right)^2 \right] \cdot dxdy \tag{5}$$

where ε_x and ε_y are the x- and y-components of the dielectric constant in the Cartesian system of coordinates and u is the electric potential. In the case of isotropic permittivity distribution ($\varepsilon = \varepsilon_x = \varepsilon_y$), Equation (5) can be rewritten as

$$F(u) = \frac{1}{2}\int_D \varepsilon \left[\left(\frac{du}{dx}\right)^2 + \left(\frac{du}{dy}\right)^2 \right] \cdot dxdy \tag{6}$$

If the effect of dielectric loss on the electric field distribution is considered, the complex functional $F(u)$ should be taken as

$$\overset{*}{F}(u)=\frac{1}{2}\int_D \omega\varepsilon_0(\varepsilon - j\varepsilon\cdot tg\delta)\left[\left(\frac{d\overset{*}{u}}{dx}\right)^2+\left(\frac{d\overset{*}{u}}{dy}\right)^2\right]dxdy \qquad (7)$$

where ω is angular frequency, ε_0 is the permittivity of free space (8.85×10^{-12} F/m), $tg\,\delta$ is tangent of the dielectric loss angle, and u^* is the complex potential.

Inside each sub-domain D_e, a linear variation of the electric potential is assumed, i.e.

$$u_e(x,y)=\alpha_{e1}+\alpha_{e2}x+\alpha_{e3}y \quad ;(e=1,2,3,..ne) \qquad (8)$$

where $u_e(x, y)$ is the electric potential of any arbitrary point inside each sub-domain D_e, α_{e1}, α_{e2} and α_{e3} represent the computational coefficients for a triangle element *e*, *ne* is the total number of triangle elements.

The calculation of the electric potential at every knot in the total network composed of many triangle elements was carried out by minimizing the function *F(u)*, that is,

$$\frac{\partial F(u_i)}{\partial u_i}=0 \quad ;i=1,2,..np \qquad (9)$$

where *np* stands for the total number of knots in the network.

Then we can get a metrical expression

$$\left[S_{ji}\right]\{u_i\}=\{T_j\} \quad i,j=1,2,..np \qquad (10)$$

where $[S_{ji}]$ is the matrix of coefficients, $\{u_i\}$ is the matrix vector of unknown values of the potential at the knots and $\{T_j\}$ is the metrical vector of free terms. The metrical equation (10) can be solved using various methods, including the Gauss–Seidel iterative method.

3.3 Implementation for FEM analysis

The basic design of a polymer insulator is as follows; A fiber reinforced plastic (FRP) core having relative dielectric constant 7.1, attached with two metal fittings, is used as the load bearing structure. Weather sheds made of HTV silicone rubber having relative dielectric constant 4.3 are installed outside the FRP core. Surrounding of the insulator is air having relative dielectric constant 1.0. AC 15 kV is energized on the lower electrode while the upper electrode connected with ground. Two dimension of the two type polymer insulators for FEM analysis are shown in Fig. 6

The whole problem domain in Fig. 6 is fictitiously divided into small triangular areas called *domain*. The potential, which is unknown throughout the problem domain, is approximated in each of these elements in terms of the potential in their vertices called *nodes*. Details of Finite Element discretization are found in [17]. The most common form of approximation solution for the voltage within an element is a polynomial approximation. PDE Tool in MATLAB is used for finite element discretization. The obtaining results are 1,653 nodes and 3,180 elements for straight sheds type insulator and 2,086 nodes and 4,030 elements for alternate sheds type insulator, respectively. The obtaining results are shown in Fig. 7

3 Simulation Results and Discussions

In this study, clean and contamination conditions are simulated using FEM via PDE Tool in MATLAB. Potential Distribution results are shown in Fig. 8 and electric field distribution are shown in Fig. 9. Comparison of potential and electric field distribution along surface of the two type polymer insulators are shown in Fig. 10 and Fig. 11, respectively. Although nonlinear potential distribution along leakage distance of the two type specimens, no significant different can be seen on the straight sheds specimen comparing with the alternate shed specimen, as shown in Fig. 10. In spite of clean condition, electric field distribution on the straight sheds specimen is slightly higher than the alternate sheds specimen as shown in Fig. 11.
Contamination condition is simulated by place 12 water droplets on the two type insulator surfaces as shown in Fig. 12 and Fig. 14. The simulation results of electric field and potential distributions are illustrated in Fig. 13 and Fig. 15, respectively. Comparison of potential and electric field distribution along surface of the two type polymer insulators are shown in Fig. 16 and Fig. 17, respectively. In case of contamination condition, although nonlinear potential distribution along leakage distance of the two type specimens, no significant different can be seen on the straight sheds specimen comparing with the alternate shed specimen, as shown in Fig. 16. However, significant different in electric field distribution can be seen the straight sheds specimen comparing with the alternate shed specimen, as shown in Fig. 17.

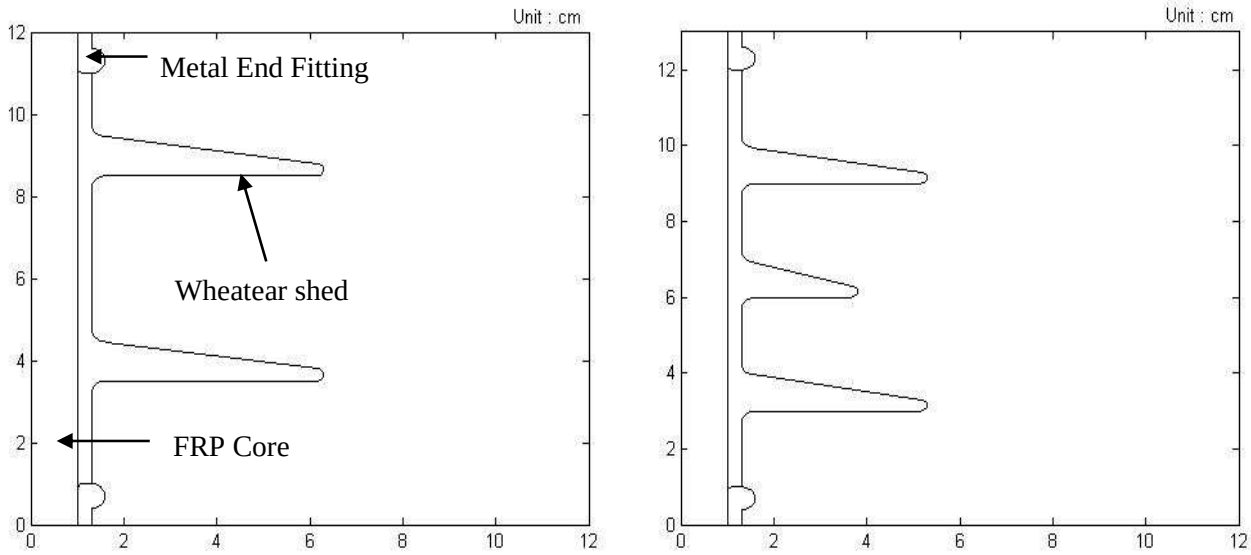

(a) Straight Sheds (b) Alternated Sheds

Fig. 6 Two Dimension of the Two Type Polymer Insulators for FEM Analysis

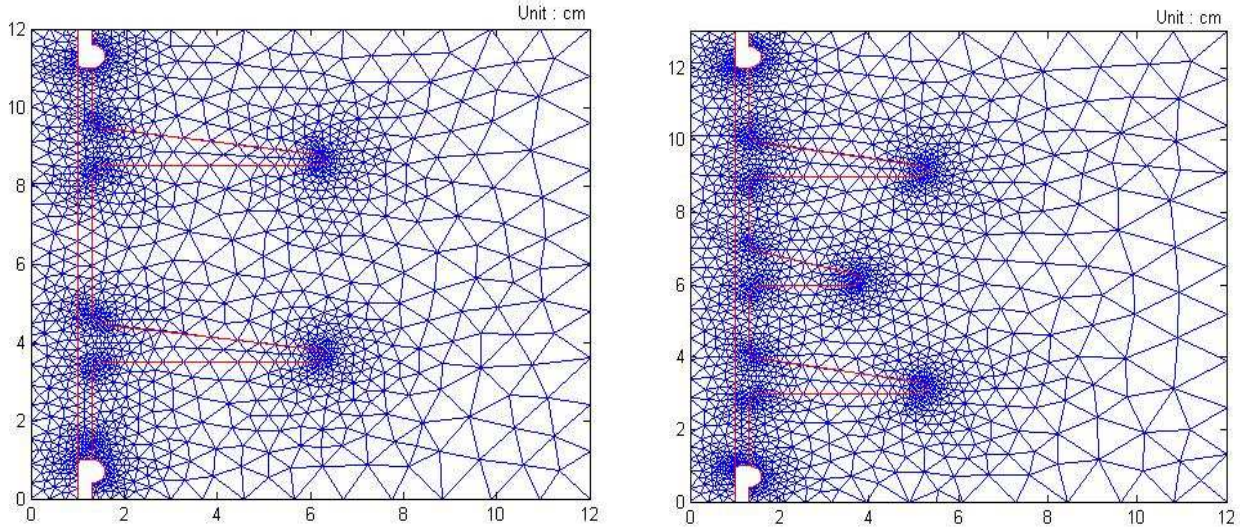

(a) Straight Sheds Insulator (b) Alternate Sheds Insulators

Fig. 7 Finite Element Discretization Results

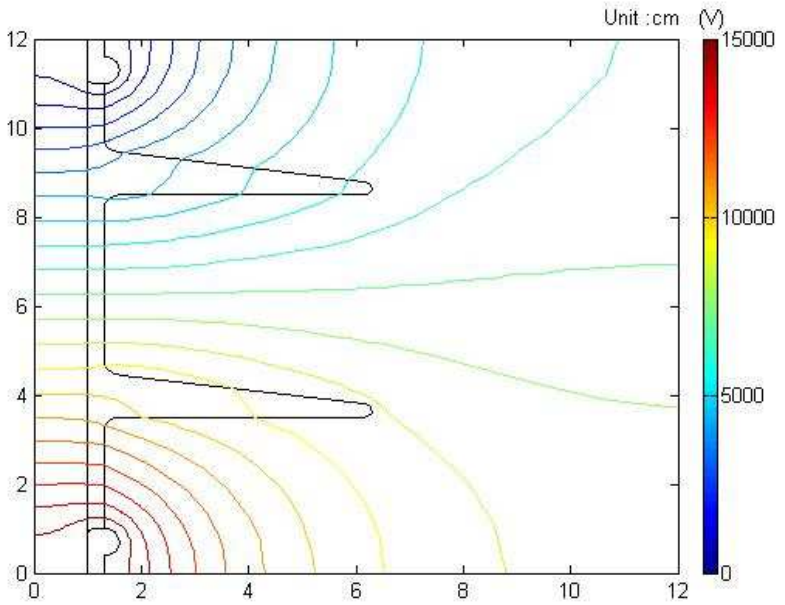

(a) Straight Sheds Insulator

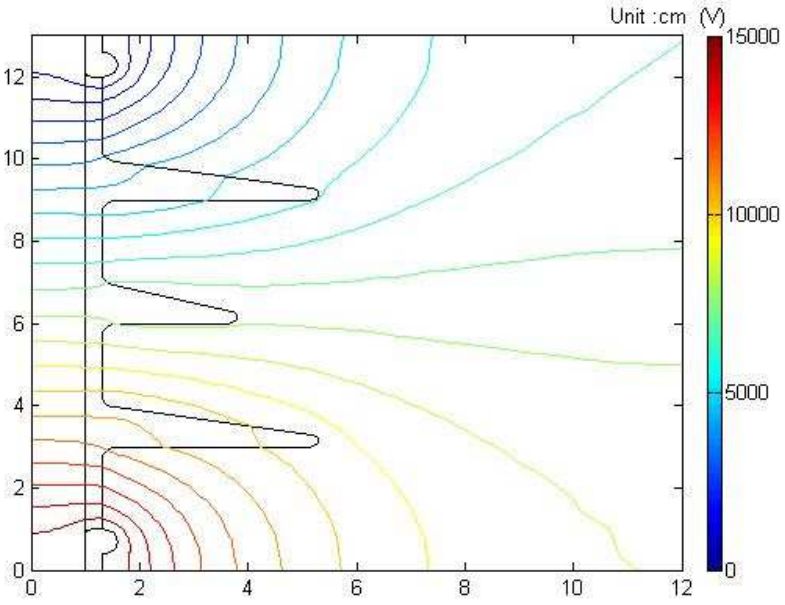

(b) Alternate Sheds Insulator

Fig. 8 Potential Distribution under Clean Condition

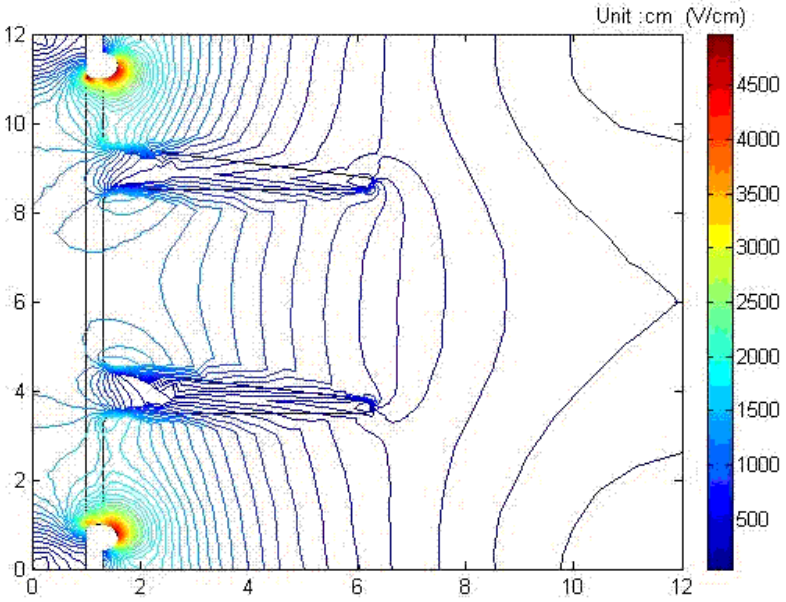

(a) Straight Sheds Insulator

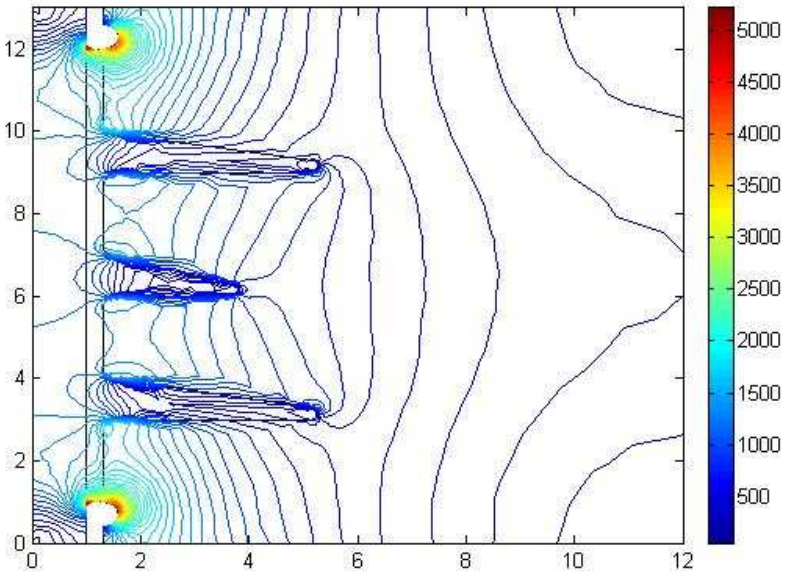

(b) Alternated Sheds Insulator

Fig. 9 Electric Field Distribution under Clean Condition

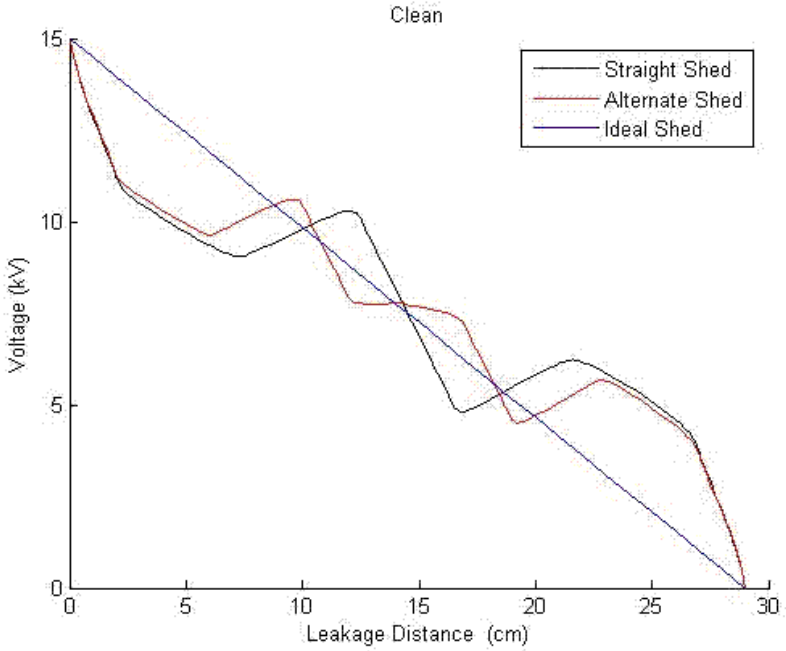

Fig. 10 Comparison of Potential Distribution

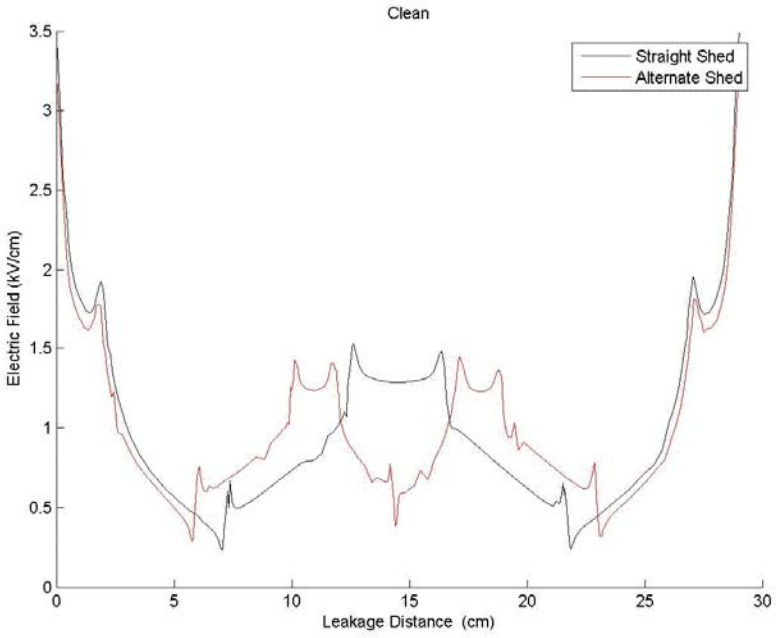

Fig. 11 Comparison of Electric Field Distribution

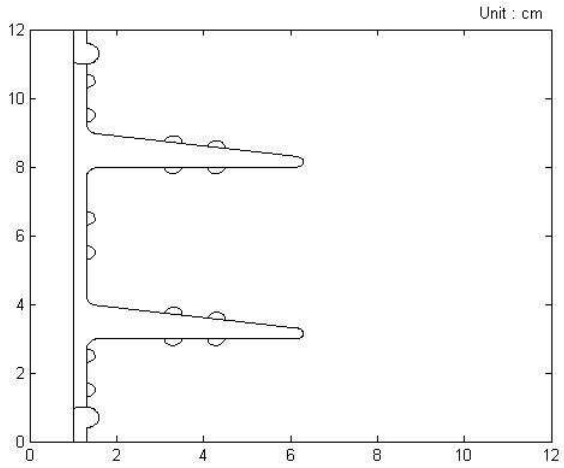

Fig. 12 Straight Sheds Insulator with Water Droplets on the Surface

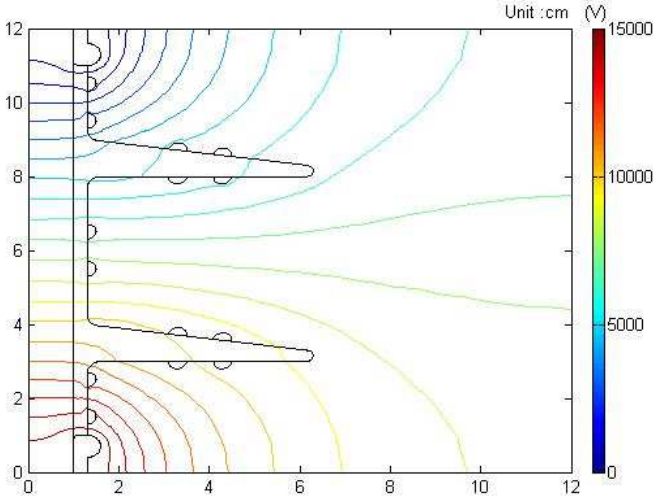

(a) Potential Distribution

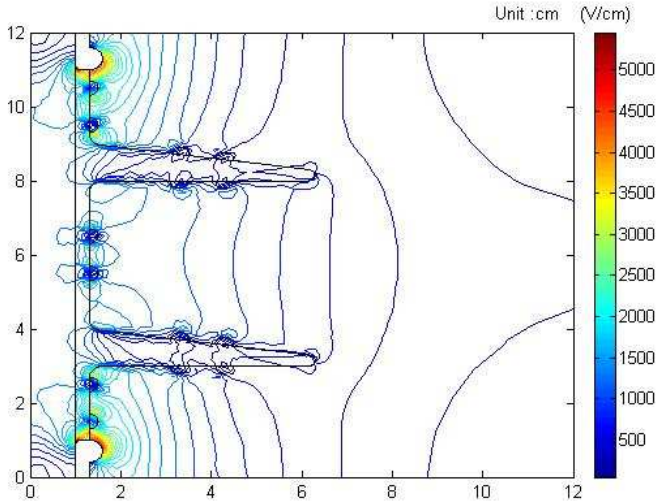

(b) Electric Field Distribution

Fig. 13 Straight sheds Insulator with Water Droplets on the Surface

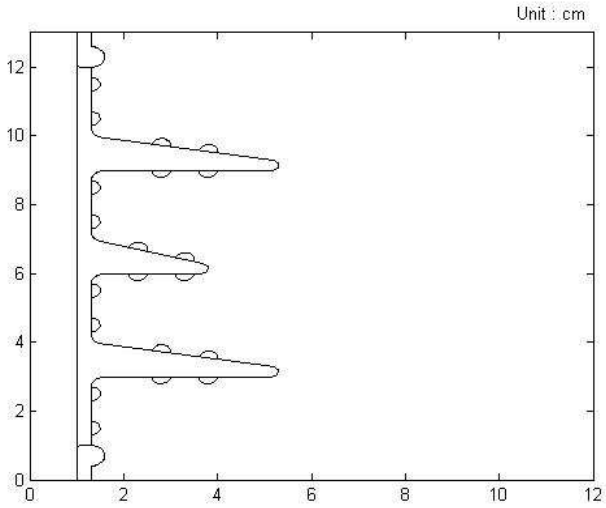

Fig. 14 Alternate Sheds Insulator with Water Droplets on the Surface

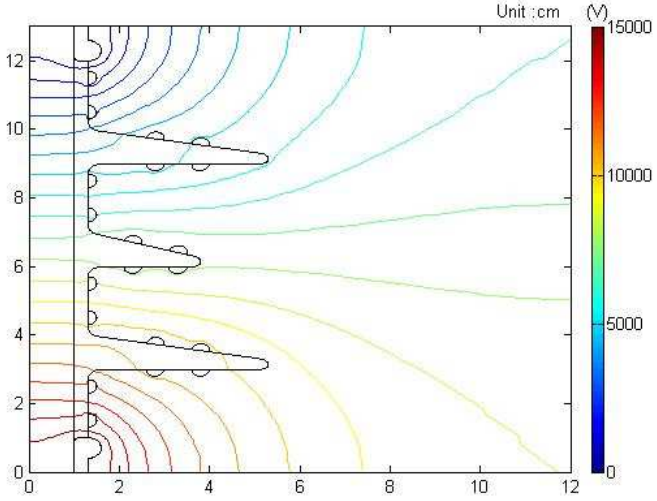

(a) Potential Distribution

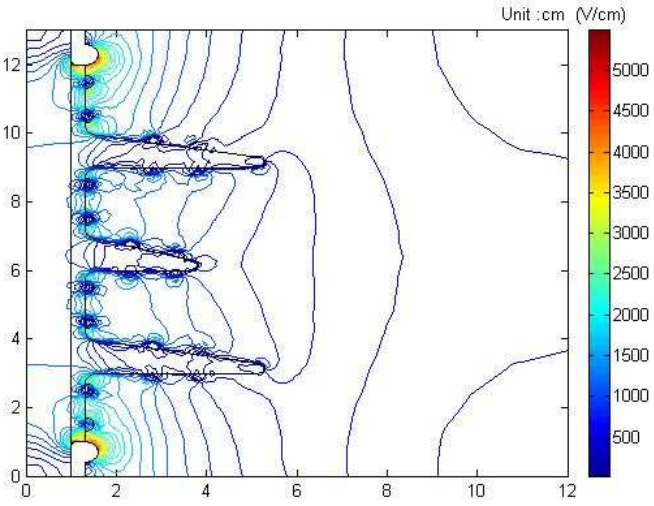

(b) Electric Field Distribution

Fig. 15 Alternate Sheds Insulator with Water Droplets on the Surface

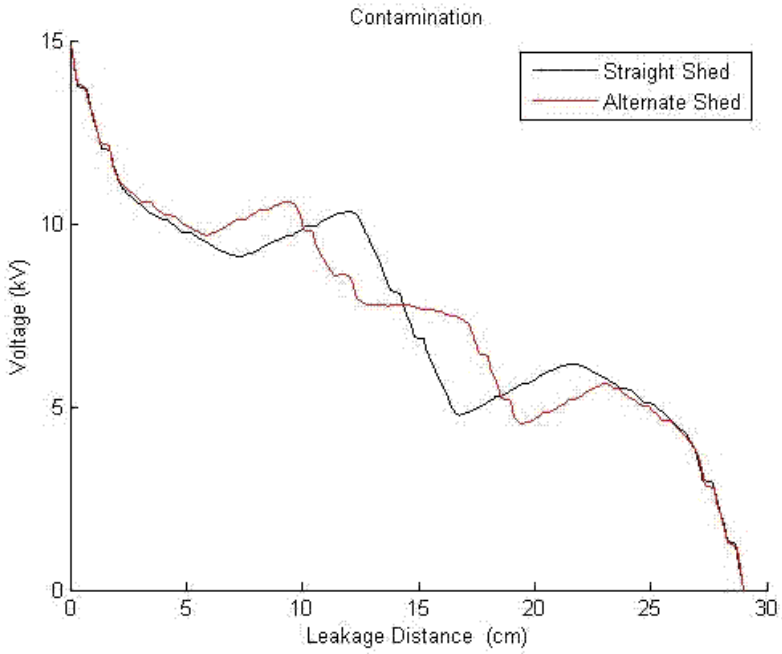

Fig. 16 Comparison of Potential Distribution under Contamination Condition

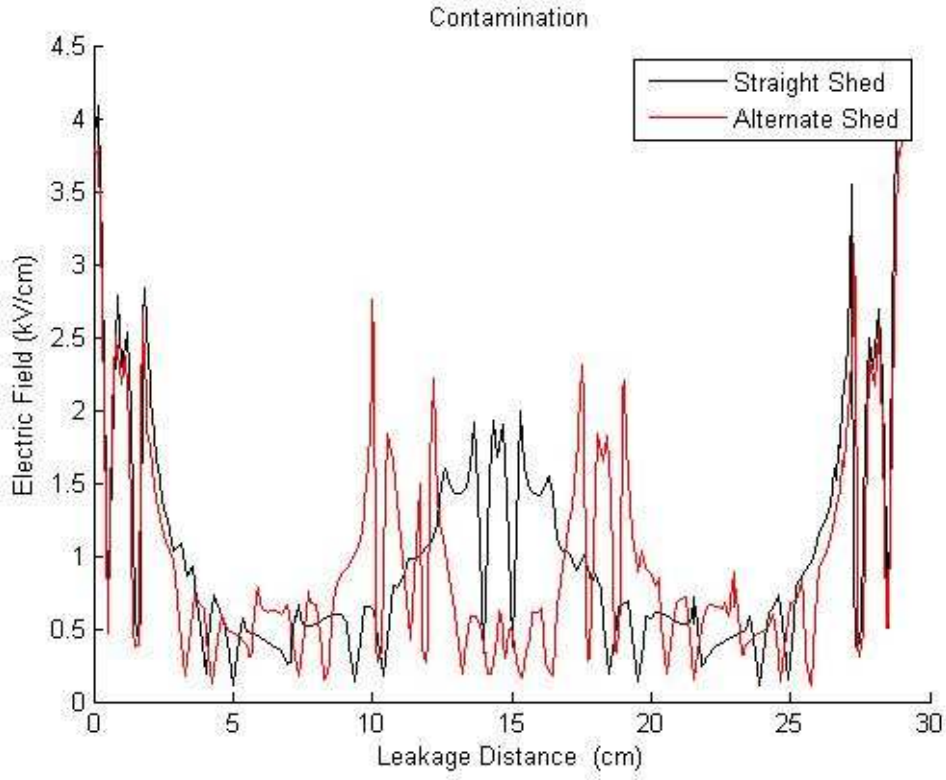

Fig. 17 Comparison of Electric Field Distribution under Contamination Condition

Under contamination condition, as illustrated in Fig. 17, significant higher electric field distribution on the trunk between sheds can be seen when comparing with the shed of the two type specimens. High magnitude of electric field can be seen on the trunk between sheds of the straight shed specimen. The simulation results are agreed with the experimental results. Higher magnitude of electric field caused more electric discharge on the insulator surface. More discharge activities caused severe surface damages. However, high magnitude of electric field also can be seen on the trunk between sheds of the alternate shed specimen but slightly erosion was obtained after 50 test cycles. The explanation may due to dry band arc discharge activies.

4 Conclusion

High magnitude of electric field distribution on the trunk between sheds of the two type polymer insulators obtained from the simulation results by using Finite Element Method. The simulation results are agreed with the experimental results. In spite of the same leakage distance and the same material, different degree of surface aging obtained from polymer insulator having different configurations.

References:

[1] CIGRE TF33.04.07, "Natural and Artificial Ageing and Pollution Testing of Polymer Insulators", *CIGRE Pub. 142*, June 1999.

[2] G. G. Karady, H. M. Schneider and F. A. M. Rizk, "Review of CIGRE and IEEE Research into Pollution Performance of Non Ceramic Insulators: Field Ageing Effects and Laboratory Test Techniques", CIGRE 1994 Session Paper No. 33 – 103, August/September 1994.

[3] I. Gutman, R. Harting, R. Matsuoka and K. Kondo, "Experience with IEC 1109 1000h Salt Fog Ageing Test for Composite Insulators", *IEEE Electrical Insulation Magazine*, Vol. 13, No. 3, May/June 1997, pp. 36 – 39.

[4] T. Zhao and R. A. Bernstorf, "Ageing Tests of Polymeric Housing Materials for Non – ceramic Insulators", *IEEE Electrical Insulation Magazine*, Vol. 14, No. 2, March/April 1998, pp. 26 – 33.

[5] R. S. Gorur, E. A. Cherney and R. Hackam, "A Comparative Study of Polymer Insulating Materials under Salt Fog Test", *IEEE Trans. on Electrical Insulation*, Vol. EI – 21, No. 2, April 1986, pp. 175 – 182.

[6] M. C. Arklove and J. C. G. Wheeler, "Salt – Fog Testing of Composite Insulators", 7th *Int. Conf. on Dielctric Material, Measurements and Applications*, Conf. Pub. No. 430, September 1996, pp. 296 – 302.

[7] S. H. Kim, R. Hackam, "Influence of Multiple Insulator Rods on Potential and Electric Field Distributions at Their Surface" , *Int. Conf. on Electrical Insulation and Dielectric Phenomena 1994*, October 1994, pp. 663 – 668.

[8] J. P Suwarno, " Investigation on Leakage Current Waveforms and Flashover Characteristics of Ceramics for Outdoor Insulators under Clean and Salt Fogs", *The WSEAS Transaction on POWER SYSTEMS*, Vol. 3, No. 6, June 2008, pp. 456 – 465.

[9] B. Marungsri, "Fundamental Investigation on Salt Fog Ageing Test of Silicone Rubber Housing Materials for Outdoor Polymer Insulators", Doctoral Thesis, Chubu University, Kasugai, Aichi, Japan, 2006.

[10] B. Marungsri, H. Shinokubo, R. Matsuoka and S. Kumagai, "Effect of Specimen Configuration on Deterioration of Silicone Rubber for Polymer Insulators in Salt Fog Ageing Test", *IEEE Trans. on DEI*, Vol. 13, No. 1 , February 2006, pp. 129 – 138.

[11] S. Sangkhasaad, "*High Voltage Engineering*", 3nd edition, Printed in Bangkok, Thailand, March 2006 (in Thai).

[12] P. Pao-La-Or, T. Kulworawanichpong, S. Sujitjorn, and S. Peaiyoung, "Distribution of flux and electromagnetic force in induction motor: a finite element approach", *The WSEAS Transaction on Systems*, Vol.5, No.3, March 2006, pp. 617 – 624.

[13] Z. L. Mahri and M. S. Rouabah, "Calculation of Dynamic Stresses using Finite Element Method and Prediction of Fatigue Failure for Wind Turbine Rotor", *The WSEAS Transaction on APPLIED and THEORETICAL MECHANICS*, Vol. 3, No. 1, January 2008, pp. 28 – 41.

[14] K. S. Ma and L. Y.Ding , "Finite element analysis of tunnel–soil–building interaction using displacement controlled model", *The WSEAS Transaction on APPLIED and THEORETICAL MECHANICS*, Vol. 3, No. 3, March 2008, pp. 73 – 82.

[15] M. Calbureanu, E. ALBOTA, R. Malciu, R. Lungu and D. Calbureanu, "Advanced Computational Concepts about Projecting a Multiple Designs of Self-Supporting Metallic Structure using Finite Element Method in Determination the Buckling Factor and Running

the Stress Analysis", *The WSEAS Transaction on APPLIED and THEORETICAL MECHANICS*, Vol. 3, No. 5, May 2008, pp. 186 – 195.

[16] C. N. Kim, J. B. Jang, X. Y. Huang, P. K. Jiang and H. Kim, "Finite element analysis of electric field distribution in water treed XLPE cable insulation (1): The influence of geometrical configuration of water electrode for accelerated water treeing test", *J. of Polymer Testing*, Vol. 26, 2007, pp. 482 – 488.

[17] P. Pao – la –or, "A New Design of Low Vibration Induction Motor using Finite Element Method", Doctoral Thesis, Suranaree University of Technology, Nakhon Ratchasima, Thailand, 2006.